

ChemComm

Accepted Manuscript



This is an *Accepted Manuscript*, which has been through the Royal Society of Chemistry peer review process and has been accepted for publication.

Accepted Manuscripts are published online shortly after acceptance, before technical editing, formatting and proof reading. Using this free service, authors can make their results available to the community, in citable form, before we publish the edited article. We will replace this *Accepted Manuscript* with the edited and formatted *Advance Article* as soon as it is available.

You can find more information about *Accepted Manuscripts* in the [Information for Authors](#).

Please note that technical editing may introduce minor changes to the text and/or graphics, which may alter content. The journal's standard [Terms & Conditions](#) and the [Ethical guidelines](#) still apply. In no event shall the Royal Society of Chemistry be held responsible for any errors or omissions in this *Accepted Manuscript* or any consequences arising from the use of any information it contains.

Pt(II)-Catalyzed Photosynthesis for H₂ Evolution Cycling Between Singly and Triply Reduced Species

 Keiya Yamamoto,^a Kyoji Kitamoto,^{ab} Kosei Yamauchi,^{ab} and Ken Sakai^{*abc}

 Received 00th January 20xx,
 Accepted 00th January 20xx

DOI: 10.1039/x0xx00000x

www.rsc.org/

A PtCl₂(bpy) derivative tethered to two viologen (MV²⁺) moieties drives photochemical H₂ evolution via forming a three-electron-reduced species possessing a bpy^{-•}-based (or MV⁰-based) reducing equivalent. Such species can only form after one electron reduction of both the MV²⁺ sites because of rapid intramolecular electron transfer from bpy^{-•} to MV²⁺.

Solar-driven water splitting into H₂ and O₂ has been studied intensively to solve the problems arising from global warming and shortage of fossil fuels.¹ In contrast with the great advancement made in the studies of purely inorganic substances,² the studies on molecular systems still require substantial advancement in order to meet the criteria required for the practical applications.^{3,4} In this context, one of our interests over the past years has been the study of Pt(II)-based molecular H₂-evolving catalysts,⁵ including those functionalized with light-harvesting chromophores, which we call 'photo-hydrogen-evolving molecular devices' (PHEMDs). The PHEMDs can be either photosensitizer-catalyst dyads consisting of a Ru(bpy)₃²⁺-derived chromophore and a Pt(II)-based H₂-evolving catalyst or even simpler mononuclear Pt(II) complexes that possess both of these functionalities.⁶ Examples of the latter Pt(II)-only systems include PV²⁺ and [PtCl₂(5,5'-MV4)]⁸⁺ depicted in Fig. 1a. These Pt(II)-only single-component photocatalysts evolve H₂ in the presence of a sacrificial electron donor (EDTA; ethylenediaminetetraacetic acid disodium salt) via two consecutive photo-driven electron transfer steps (Z-scheme photosynthesis) leading to the formation of a two-electron-reduced species (PHEMD²⁻) which can thermally drive H₂ evolution from water (see Fig. 1b).⁷ In these studies, a singly reduced species (PHEMD^{-•}) is first generated via reductive quenching of the photoexcited state

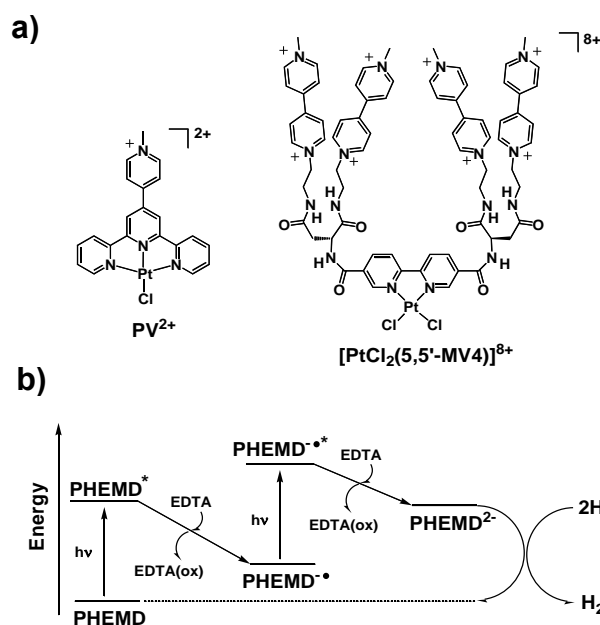


Fig. 1 a) Examples of PHEMDs. b) Z-scheme photosynthesis by a PHEMD.

(PHEMD^{*}) by EDTA, followed by photoexcitation of PHEMD^{-•} leading to a second reduction via the reaction: PHEMD^{-••} + EDTA → PHEMD²⁻ + EDTA(ox), where the asterisked species corresponds to its photoexcited state. An important feature is that the one-electron-reduced species cannot thermally drive H₂ evolution from water.^{7a} Thus, H₂ is generated via photochemical activation of the one-electron-reduced species.

Here we report on a new PtCl₂(bpy) derivative (bpy = 2,2'-bipyridine) tethered to two pendant viologen unit, [PtCl₂(bpyMV2)]⁴⁺ in Fig. 2a. This system is found to drive photochemical H₂ evolution only via formation of three-electron-reduced species as illustrated in Figs. 2b,3. Importantly, this molecular system does not consume the initially collected one-electron when it photocatalyzes H₂ evolution from water. Thermal paths HER(1) and HER(2) do not take place, while either path HER(3) or HER(4) may take place. Thus we will show that a reducing

^a Department of Chemistry, Faculty of Sciences, Kyushu University, 6-10-1 Hakozaki, Higashi-ku, Fukuoka 812-8581, Japan. E-mail: ksakai@chem.kyushu-univ.jp

^b International Institute for Carbon-Neutral Energy Research (WPI-I2CNER), Kyushu University, Motoooka 744, Nishi-ku, Fukuoka 819-0395, Japan.

^c Center for Molecular Systems (CMS), Kyushu University, Motoooka 744, Nishi-ku, Fukuoka 819-0395, Japan.

† Electronic Supplementary Information (ESI) available. See DOI: 10.1039/x0xx00000x

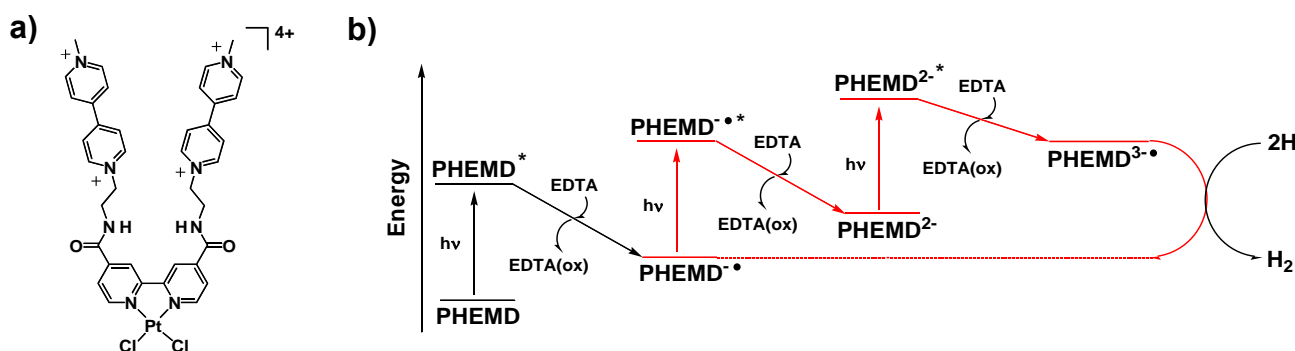


Fig. 2 a) Structure of $[\text{PtCl}_2(\text{bpyMV}_2)]^{4+}$. b) Photochemical H_2 evolution cycling between singly and triply reduced $[\text{PtCl}_2(\text{bpyMV}_2)]^{4+}$.

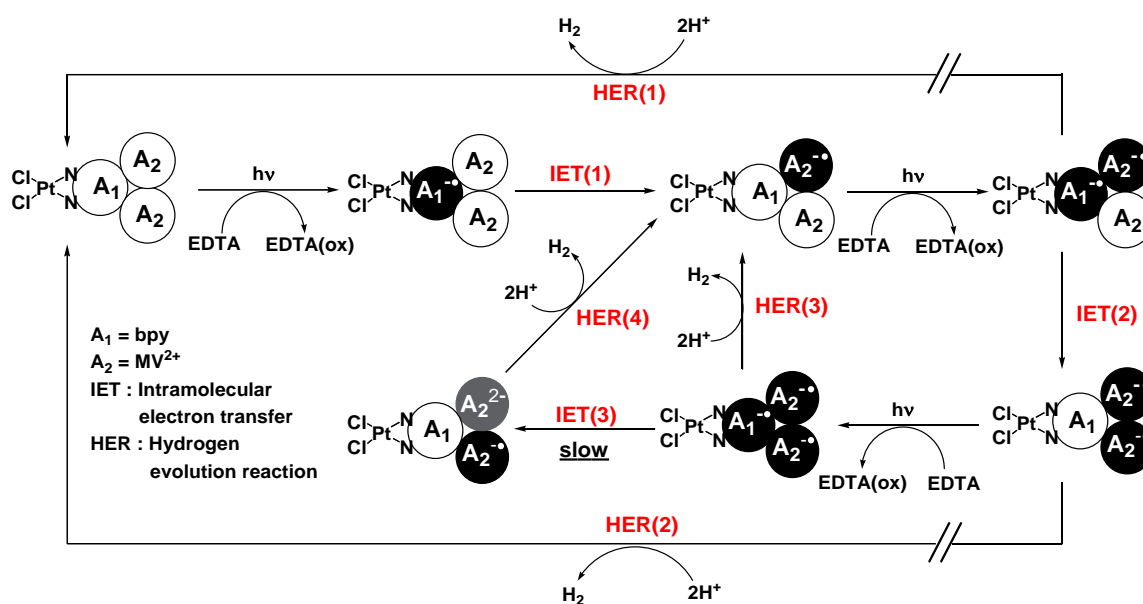


Fig. 3 Reaction model of $[\text{PtCl}_2(\text{bpyMV}_2)]^{4+}$.

equivalent stored over the bpy ligand is important to drive water reduction to H_2 . In other words, the photocatalytic H_2 evolution cycle can be 'switched on' only after filling both the pendant viologen acceptors with a reducing equivalent.

As previously reported for $[\text{PtCl}_2(5,5'\text{-MV}_4)]^{8+,7b,8}$ the $\text{PtCl}_2(\text{bpy})$ chromophore possesses a metal-to-ligand charge transfer ($^1\text{MLCT}$) band at 388 nm (Fig. S1), which can be used to generate a triplet excited state ($^3\text{MLCT}$ state) that can be reductively quenched by a sacrificial electron donor present in solution. $[\text{PtCl}_2(\text{bpyMV}_2)]^{4+}$ does not exhibit emission at room temperature in aqueous solution. However, an emission in the range 500-700 nm is observed for $[\text{PtCl}_2(\text{bpyMV}_2)]^{4+}$ in a methanol/ethanol/*N,N*-dimethylformamide (MED; 4:4:1) glass at 77 K with the 0-0 and 0-1 vibronic emission peaks respectively centred at 496 and 533 nm with an average lifetime being $\langle \tau \rangle = 3.14 \mu\text{s}$ (see Fig. S3). This long-lived character together with the large Stokes shift (ca. 150 nm) reveals that the emission arises from the triplet.

Electrochemical study reveals that the first and second reductions of $[\text{PtCl}_2(\text{bpyMV}_2)]^{4+}$ occur at -0.80 and -1.20 V vs. Fc/Fc^+ (Fig. S4), assignable to the $\text{MV}^{2+}/\text{MV}^{•+}$ and $\text{MV}^{•+}/\text{MV}^0$ couples, respectively. These assignments are unambiguous based on the values reported for the series of $\text{PtCl}_2(\text{bpy})-(\text{MV}^{2+})_n$ ($n = 2, 4$) dyads.^{7b} The third reduction peak is observed at -1.30 V vs. Fc/Fc^+ and is assignable to the $\text{bpy}/\text{bpy}^{•-}$ couple (Fig. S4). These redox properties show that the

driving force for the water reduction by a $\text{MV}^{•+}$ -based reducing equivalent is lower than those by the $\text{bpy}^{•-}$ - and MV^0 -based reducing equivalents by 0.5 and 0.4 eV, respectively. This is correlated with our major finding that the $\text{bpy}^{•-}$ -based (or MV^0 -based) reducing equivalent must be involved to drive photocatalytic H_2 formation with this system.

Next, we focus on the photo-driven electron storage behaviour of $[\text{PtCl}_2(\text{bpyMV}_2)]^{4+}$ in the presence of EDTA. As previously observed for the series of $\text{PtCl}_2(\text{bpy})-(\text{MV}^{2+})_n$ dyads,^{7b} photoirradiation of $[\text{PtCl}_2(\text{bpyMV}_2)]^{4+}$ results in growth of bands in the visible to near-infrared region (Fig. 4a). The broad absorption features appearing above 800 nm are characteristic of those derived from the $(\text{MV}^{•+})_2$ π -dimer species (i.e., $[\text{PtCl}_2(\text{bpy})-(\text{MV}^{•+})_2]^{2+}$).⁹ The geometrical and electronic structures of $[\text{PtCl}_2(\text{bpy})-(\text{MV}^{•+})_2]^{2+}$ were computed for both closed-shell and open-shell singlet states, in which a closed-shell singlet state turned out to be a unique solution for this two-electron-reduced system. The optimized geometry of $[\text{PtCl}_2(\text{bpy})-(\text{MV}^{•+})_2]^{2+}$ (singlet) has a structure in which two singly reduced viologen planes are stacked intramolecularly in a staggered fashion (Fig. S5). Absorption features simulated using the TD-DFT results (Fig. S10) are somewhat consistent with the observed spectral features. Formation of this $(\text{MV}^{•+})_2$ π -dimer species saturates after around 10 min irradiation. The molar absorptivity of the two-electron-reduced

species at 353 nm ($\epsilon_{353} = 24000 \text{ M}^{-1}\text{cm}^{-1}$) was independently determined by adding a large excess of $\text{Na}_2\text{S}_2\text{O}_4$ (see Fig. S6). This absorptivity value was used to calibrate the number of electrons stored per molecule, which corresponds to the vertical axis in Fig. 4b. The results reveal that approximately two electrons are stored per molecule under steady-state conditions. Moreover, the two-electron-reduced species generated in the above experiments shows only a minor decay over 1 h and does not exhibit a considerable decay over 15 h when it is left at 20 °C in the dark under Ar (see Fig. S7), indicating that thermal reduction of water by this species ($[\text{PtCl}_2(\text{bpy})-(\text{MV}^+)_2]^{2+} + 2\text{H}^+ \rightarrow [\text{PtCl}_2(\text{bpy})-(\text{MV}^{2+})_2]^{4+} + \text{H}_2$) is not a major path to H_2 evolution. As previously reported,^{5c} electrochemically generated non-tethering free MV^{2+} does bleach in the presence of $\text{PtCl}_2(\text{dcbpy})$ (dcbpy = 4,4'-dicarboxy-2,2'-bipyridine) due to the occurrence of thermal H_2 evolution reaction catalysed by $\text{PtCl}_2(\text{dcbpy})$ (see Fig. S13). This is correlated with the fact that the redox potential of $(\text{MV}^+)_2/\text{MV}^{2+}$ is 0.15 V positive-shifted compared to that of the free MV^{2+} species, as reported ($E_{1/2}((\text{MV}^+)_2/(\text{MV}^{2+})) = -0.55 \text{ V vs. SCE}$; $E_{1/2}(\text{MV}^+/\text{MV}^{2+}) = -0.70 \text{ V vs. SCE}$).¹⁰

Photochemical H_2 evolution by $[\text{PtCl}_2(\text{bpyMV}_2)]^{4+}$ in the presence of EDTA is shown in Fig. 5a. The turnover number (TON)

reaches 18 after 24-h irradiation. Importantly, the H_2 evolution rate remains nearly constant within 24 h, showing that this molecular photocatalyst is relatively stable. Note that viologen tethers are essential to enhance the H_2 -evolving activity of such $\text{PtCl}_2(\text{bpy})$ derivatives, since photoirradiation of $\text{PtCl}_2(\text{dcbpy})$ and EDTA does not lead to H_2 evolution.^{7b} In situ dynamic light scattering (DLS) measurements were also carried out to check for colloidal platinum formation. The light scattering intensity during the photocatalysis using $[\text{PtCl}_2(\text{bpyMV}_2)]^{4+}$ at first increases due to dispersion of unidentified particles (Fig. S8 red). However, upon exposure of the resultant solution to air, the light scattering intensity abruptly decreases and the initial blank level of scattering intensity can be recovered (see Fig. S8 blue). Therefore, the observed dispersion during the photolysis must be caused by partial precipitation of some reduced forms of $[\text{PtCl}_2(\text{bpyMV}_2)]^{4+}$ that have lower solubility in aqueous media. Precipitation of such reduced species has often been observed in our previous studies.⁶ⁱ These observations clearly rule out colloidal platinum formation under our photolysis conditions.

Importantly, we observe quite clear ON-OFF behaviour for H_2 generation upon turning ON and OFF the light irradiation (see Fig. 5b). As discussed above for Fig. 4, the major chemical species in solution

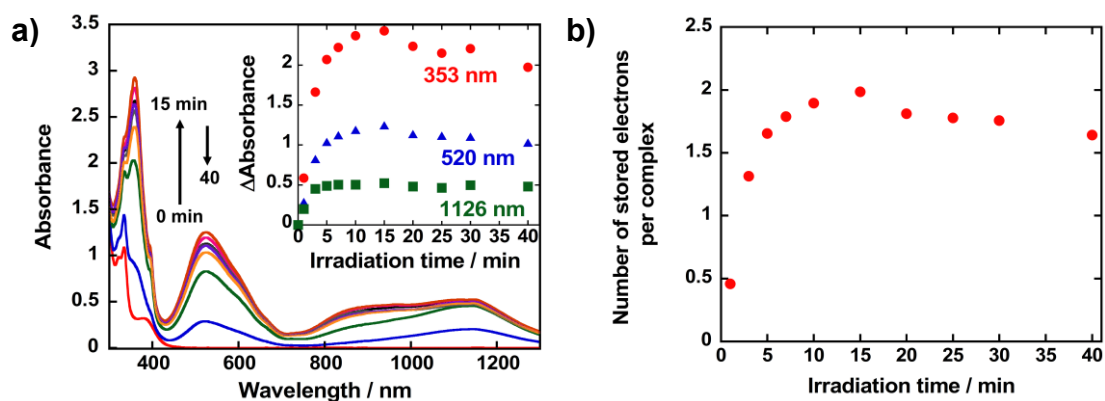


Fig. 4 a) Spectral changes during the photolysis of an aqueous acetate buffer solution (pH 5.0; at 20 °C under Ar) containing 0.1 mM $[\text{PtCl}_2(\text{bpyMV}_2)]^{4+}$, 0.1 M NaCl, and 30 mM EDTA. Inset: Absorbance changes at 353 nm (red), 520 nm (blue), and 1126 nm (green) during photolysis. b) Changes in the total number of electrons stored over $[\text{PtCl}_2(\text{bpyMV}_2)]^{4+}$ during photolysis shown in Fig. 4a.

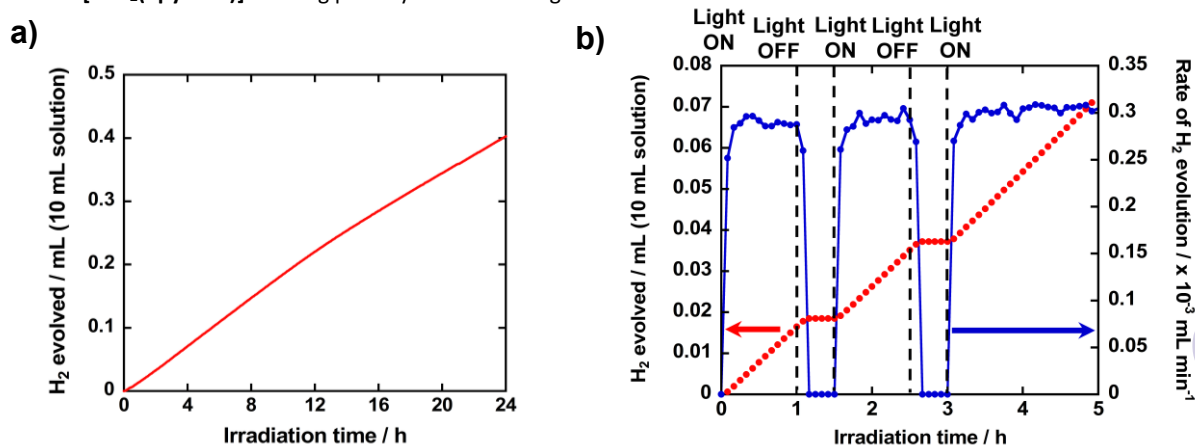


Fig. 5 a) Photochemical H_2 production from an aqueous acetate buffer solution (pH 5.0, 10 mL; at 20 °C under Ar) containing 0.1 mM $[\text{PtCl}_2(\text{bpyMV}_2)]^{4+}$, 0.1 M NaCl, and 30 mM EDTA. b) Photoresponse of H_2 production. Red and blue dots correspond to the amount of H_2 evolved and the rate of H_2 evolution, respectively, where experimental conditions are the same as those in Fig. 5a.

is a two-electron-reduced species at each light-off time shown in Fig. 5b, which re-confirms that thermal reduction of water by $[\text{PtCl}_2(\text{bpy})-(\text{MV}^+)_2]^{2+}$ does not proceed under these conditions. As a result, we can conclude that the observed H_2 evolution results from the photoexcitation of the two-electron-reduced species. This has a similarity to the H_2 evolution via two consecutive photo-driven electron transfer steps discovered for PV^{2+} in which photoexcitation of PV^{*+} is essential to generate the doubly reduced species (PV^0) which thermally reduces water to H_2 .^{7a} With $[\text{PtCl}_2(\text{bpyMV}_2)]^{4+}$, photoexcitation of the two-electron-reduced species obviously plays a major role in generating species that drives thermal H_2 evolution from water. We now assume that **HER(3)** predominates **HER(4)** because of the slower nature of **IET(3)** (lower driving force for this IET; $\Delta G_{\text{IET}} = -0.1$ eV; see Fig. S4) as well as the lower driving force for the H_2 evolution via **HER(4)**. The initial minor decay of reduced species seen in Fig. S7b might correspond to the occurrence of **HER(4)**. Nevertheless, the more detailed studies are needed to further clarify this observation.

Our above results indicate that $[\text{PtCl}_2(\text{bpyMV}_2)]^{4+}$ is a unique system which can only drive H_2 evolution via formation of three-electron-reduced species which include a $\text{bpy}^{\bullet-}$ -based (or MV^0 -based) reducing equivalent, as illustrated with path **HER(3)** (or **HER(4)**). Possibly, this is due to the close location of MV^{2+} with regard to the bpy moiety, which enables rapid intramolecular electron transfer from $\text{bpy}^{\bullet-}$ to one of the adjacent MV^{2+} units, if there is any un-reduced MV^{2+} site. In other words, the **IET(2)** step in Fig. 3 is much faster than the competing H_2 evolution path **HER(1)**. On the contrary, we assume that the $[\text{PtCl}_2(5,5'\text{-MV}_4)]^{8+}$ family can adopt the thermal path **HER(1)** since they can photocatalyze H_2 evolution while a portion of the multiple MV^{2+} sites remain un-reduced, presumably due to the slower nature of both the **IET(1)** and **IET(2)** steps.^{7b} As a result, we conclude that all the MV^{2+} sites in $[\text{PtCl}_2(\text{bpyMV}_2)]^{4+}$ must be reduced in order to generate a $\text{bpy}^{\bullet-}$ (or MV^0) site required to drive the H_2 evolution process.

Finally we note that the quantum yield of H_2 formation is relatively low for the present system ($\Phi(0.5\text{H}_2) = 0.02\%$; Figs. S11,12). This is likely due to quenching of the $\text{PtCl}_2(\text{bpy})$ -based $^3\text{MLCT}$ state by the $(\text{MV}^+)_2$ π -dimer moiety in close proximity, as demonstrated by the complete quenching of emission from $[\text{PtCl}_2(\text{bpy})-(\text{MV}^+)_2]^{2+}$ in a frozen media at 77 K (Fig. S14). Extended studies are still ongoing in our laboratory.

This work was Supported by a Grant-in-Aid for Scientific Research (B) (No. 24350029), and a Grant-in-Aid for Scientific Research on Innovative Areas 'Artificial Photosynthesis' (Nos. 2406, 24107004) from the Ministry of Education, Culture, Sports, Science, and Technology (MEXT) of Japan. This was further supported by the International Institute for Carbon Neutral Energy Research (WPI-I2CNER), sponsored by the World Premier International Research Center Initiative (WPI), MEXT, Japan. K.K. acknowledges Research Fellowships of the Japan Society for the Promotion of Science for Young Scientists.

Notes and references

1. A. J. Esswein and D. G. Nocera, *Chem. Rev.*, 2007, **107**, 4022.
2. (a) A. Kudo and Y. Miseki, *Chem. Soc. Rev.*, 2009, **38**, 253; (b) K. Sayama, K. Mukasa, R. Abe, Y. Abe and H. Arakawa, *Chem. Commun.*, 2001, 2416; (c) K. Maeda, K. Teramura, D. Lu, T. Takata, N. Saito, Y. Inoue and K. Domen, *Nature*, 2006, **440**, 295.
3. (a) M. Wang, L. Chen and L. Sun, *Energy Environ. Sci.*, 2012, **5**, 6763; (b) Z. Han, W. R. McNamara, M.-S. Eum, P. L. Holland and R. Eisenberg, *Angew. Chem. Int. Ed.*, 2012, **51**, 1667; (c) B. Mat. J. Fize, J. Moussa, H. Amouri, A. Pereira, V. Artero, G. Izzet and A. Proust, *Energy Environ. Sci.*, 2013, **6**, 1504; (d) S. Losse, J. G. Vos and S. Rau, *Coord. Chem. Rev.*, 2010, **254**, 2492; (e) H. L. W. Guo, K. Wu, Z. Chen, J. Bacsa, D. G. Musaev, Y. V. Geletii, S. M. Lauinger, T. Lian and C. L. Hill, *J. Am. Chem. Soc.*, 2014, **136**, 14015; (f) T. Stoll, M. Gennari, J. Fortage, C. E. Castillo, M. Rebarz, M. Sliwa, O. Poizat, F. Odobel, A. Deronzier and M.-L. Collomb, *Angew. Chem. Int. Ed.*, 2014, **53**, 1654.
4. (a) L. Duan, F. Bozoglian, S. Mandal, B. Stewart, T. Privalov, A. Llobet and L. Sun, *Nat. Chem.*, 2012, **4**, 418; (b) D. J. Wasylenk., R. D. Palmer and C. P. Berlinguette, *Chem. Commun.*, 2013, **40**, 218; (c) J. J. Concepcion, D. K. Zhong, D. J. Szalda, J. M. Muckerman and E. Fujita, *Chem. Commun.*, 2015, **51**, 4105; (d) J. J. Concepcion, M.-K. Tsai, J. T. Muckerman and T. J. Meyer, *J. Am. Chem. Soc.*, 2010, **132**, 1545; (e) L. Kohler, N. Kaveevivitchai, R. Zong and R. P. Thummel, *Inorg. Chem.*, 2011, **50**, 912; (f) L. Wang, M. Mirmohades, A. Brown, L. Duan, F. Li, C. Daniel, R. Lomoth, L. Sun and L. Hammarström, *Inorg. Chem.*, 2015, **54**, 2742.
5. (a) H. Ozawa, Y. Yokoyama, M. Haga and K. Sakai, *Dalton Trans.*, 2007, 1197; (b) K. Sakai and H. Ozawa, *Coord. Chem. Rev.*, 2008, **251**, 2753. (c) K. Yamauchi, S. Masaoka and K. Sakai, *J. Am. Chem. Soc.*, 2009, **131**, 8404.
6. (a) H. Ozawa, M. Haga and K. Sakai, *J. Am. Chem. Soc.*, 2006, **128**, 4926; (b) S. Masaoka, Y. Mukawa and K. Sakai, *Dalton Trans.*, 2010, **39**, 5868; (c) H. Ozawa, M. Kobayashi, B. Balan, S. Masaoka and K. Sakai, *Chem. Asian J.*, 2010, **5**, 1860; (d) M. Hirahara, S. Masaoka and K. Sakai, *Dalton Trans.*, 2011, **40**, 3967; (e) H. Ozawa and K. Sakai, *Chem. Commun.*, 2011, **4**, 2227; (f) G. Ajayakumar, M. Kobayashi, B. Balan, S. Masaoka and K. Sakai, *Dalton Trans.*, 2011, **40**, 3955; (g) C. V. Sunees', B. Balan, H. Ozawa, Y. Nakamura, T. Katayama, M. Muramatsu, Y. Nagasawa, H. Miyasaka and K. Sakai, *Phys. Chem. Chem. Phys.*, 2014, **16**, 1607; (h) R. Okazaki, S. Masaoka and K. Sakai, *Dalton Trans.*, 2009, 6127; (i) K. Yamauchi and K. Sakai, *Dalton Trans.*, 2015, **44**, 8685.
7. (a) M. Kobayashi, S. Masaoka and K. Sakai, *Angew. Chem. Int. Ed.*, 2012, **51**, 7431; (b) K. Kitamoto and K. Sakai, *Angew. Chem. Int. Ed.*, 2014, **53**, 4618.
8. M. Ogawa, G. Ajayakumar, S. Masaoka, H.-B. Kraatz and K. Sakai, *Chem. Eur. J.*, 2011, **17**, 1148.
9. C. Lee, Y. M. Lee, M. S. Moon, S. H. Park, J. W. Park, K. G. Kim and S.-J. Jeon, *J. Electroanal. Chem.*, 1996, **416**, 139.
10. W. S. Jeon, H.-J. Kim, C. Lee and K. Kim, *Chem. Commun.*, 2007, 1828.